ICEE 2020 1570693276

Polyaniline Nanofibers as Chemiresistive Transducers: Seeded Synthesis, Characterization and DNA Sensing

Suryasnata Tripathy[1], Rahul Gangwar[2], Siva Rama Krishna Vanjari[3], Shiv Govind Singh*
Department of Electrical Engineering
Indian Institute of Technology, Hyderabad, India- 502285
[1]suryasnata.tripathy@gmail.com, [2]ee18resch11019@iith.ac.in, [3]svanjari@ee.iith.ac.in, *sgsingh@ee.iith.ac.in
*Corresponding Author

***Abstract*—In this paper, seeded synthesis of Polyaniline (PANi) nanofibers, their characterization and use as transducers in chemiresistive DNA sensing have been reported. PANi, among many one-dimensional conductive polymers, has shown great potential as a transducer in chemiresistive biosensing in general and DNA sensing in particular, on account of its natural conductivity, ease of doping and surface functionalization. Herein, PANi nanofibers were synthesized using a seeding method, using single walled carbon nanotube (SWCNT) seeds. Surface morphology of the thus synthesized nanofibers were investigated using scanning electron microscopy (SEM) and transmission electron microscopy (TEM). The nanofibers were surface modified with 2% glutaraldehyde for facilitating probe-DNA immobilization, and the results of the same were investigated using Fourier transform infrared spectroscopy. Further, towards analyzing the electrical transport properties of the PANi nanofibers, I-V characteristics were recorded in the applied bias range of -10 V - +10 V, using Agilent B1500A parametric analyzer. As inferred, the I-V response was symmetric about the vertical axis, revealing a crossover between near-Ohmic and power-law dominated regions. As a case study, in this work, the PANi nanofibers were used as transducers for chemiresistive detection of Dengue virus specific consensus primers (DENVCP).**

Keywords—DNA Sensors, PANi, Chemiresistive, Seeded synthesis, 1-D nanofibers, Hybridization.

I. Introduction

DNA hybridization detection is of significant importance in healthcare and genetics, as it finds plausible applications in the diagnosis of harmful mutation and infectious diseases [1-4]. Further, identification of microbial and viral DNA / RNAs has greatly influenced fields such as food adulteration [5-6], water/soil analysis [7] and disease diagnosis. Also, the ability to accurately identify wildtype and mutant DNAs via hybridization detection can allow one to gather, and interpret, genetic information having far-fetched implications.

In general, DNA hybridization sensors, targeting either wildtype or mutated targets, make use of single stranded nucleotide probes anchored on to sensor surfaces, that are complementary to the target nucleotide. Such probes are often designed with specific labels at one end, such as fluorophores, redux-active species and nanoparticles, which help transduce the target nucleotide hybridization, by generating / amplifying the corresponding response signal. On account of the type of signals that get recorded in response to and in tandem with the hybridization event, several transduction principles have emerged over the years, leading to the development of a myriad of DNA sensors [8-9]. In the past, our group has also reported the development of several electrochemical and chemiresistive biosensors targeting DNA hybridization / mutation detection, involving metal oxide nanomaterials and conductive polymers [10-15]. In this work, we discuss about the development of Polyaniline (PANi) nanostructure based chemiresistive platform, targeting DNA hybridization detection.

PANi, being a conductive polymer in its protonated emeraldine form, is highly suitable for chemiresistive biosensing applications, based on its high propensity to doping, and ease of surface modification. In contrast to our previous works involving PANi based sensors that included direct electrospinning of composite nanofibers [11,14], herein, we have adopted a wet-chemical approach for the nanomaterial synthesis. Also, the mode of nanomaterial deposition on to the sensor platforms is dropcasting, as opposed to the direct electrospinning method. In here, we have further analysed the current-voltage characteristics of the dropcasted PANi nanofiber networks. As explained in detail later in this communication, the I-V characteristics of the said nanofiber network is partly linear ($I \alpha V$) at lower values of the applied bias, and is mostly nonlinear ($I \alpha V^n$). This inherent non-linearity is somewhat inconvenient in developing chemiresistive platforms, that rely on calculating the overall resistance of the fiber-network for the desired transduction. This inconvenience is related to the fact that the applied voltage corresponding to the onset of this nonlinearity, and the extent of non-linearity (i.e. the exact value of n, for $I \alpha V^n$), may not necessarily remain constant for a given fiber network, before and after target hybridization, making the comparative analysis difficult. To avoid this, we have strategically limited the resistance calculations to the linear (near-Ohmic) range of the I-V characteristics.

In this work, as a case study, detection of Dengue virus specific consensus primer (DENVCP) is reported. The consensus primer, as reported previously in [10], is a representative sequence for all the 4 known serotypes of the Dengue virus. In the subsequent sections of this manuscript, particulars concerning the nanofiber synthesis and its characterization, protocols associated with the sensor development and results specific to the targeted application are described in detail.

II. Methods

A. Synthesis of PANi Nanofibers

The nanofiber seeding based synthesis of PANi nanofibers was carried out using a protocol, as described previously in [16]. In brief, 0.782 g of Aniline was added to 60 mL of 1 M HCl, along with 2 mg of single walled carbon nanotubes (SWCNT). The CNTs were added in the mixture as the seed template, for the desired nanofiber synthesis. To this solution,

978-1-7281-8660-3/20/$31.00 @2020 IEEE

2020 5th IEEE International Conference on Emerging Electronics (ICEE) | 978-1-7281-8660-3/20/$31.00 ©2020 IEEE | DOI: 10.1109/ICEE50728.2020.9776939

a mixture of 0.365 g Ammonium peroxydisulphate and 80 mL HCl was added subsequently, and the mixture was allowed to rest for 2 hours. The dark green precipitate was then filtered, repeatedly washed and dried (at 80 ºC, for 12 hours), so as to obtain the desired PANi nanofibers. All the chemicals used in this work were purchased from Sigma Aldrich, USA. For all experimental purposes, DI water from a Millipore water purifier system was used.

B. Electrode Fabrication

For this work, interdigitated microelectrodes were fabricated using standard CMOS technology, following a protocol as described in [14]. Briefly, following standard cleaning protocol, oxidized p-type Si wafers were subjected to metal deposition (Ti/Au: 20/80 nm) via e-beam evaporation. Afterwards, optical photolithography was performed using a positive photoresist and a printed photomask, towards pattern ttransfer. The substrates were subsequently subjected to metal etching for removal of the unwanted metal, following which the photoresist layer was removed in acetone, so as to realize the interdigitated designs. The as-fabricated interdigitated electrodes were characterized by a metallic finger-width and an inter-finger distance of 200 and 80 microns, respectively [14].

C. Sensor protocols

Towards preparing the chemiresistive devices, the wet-chemically synthesized PANi nanofibers were first dispersed in ethanol, via ultrasonication. This step is critical to obtain a homogeneous dispersion. On to the interdigitated electrodes, 1.5 µL of the said fiber dispersion was then dropcasted manually, following a shadow-masking assisted protocol, as described previously in [14]. In this case, post nanofiber dropcasting, the devices were dried at 40 ºC for 2 hours to facilitate the removal of solvent. Here, any high temperature treatment was avoided intentionally, as properties of PANi are highly sensitive to thermal treatment. Desired surface modification of PANi nanofibers was later accomplished by incubating the nanofibers in 2 % glutaraldehyde solution (v/v, in DI water) for 4 hours at 25 ºC. Subsequently, the functionalized nanofibers were treated with a 1:1 mixture of NHS and EDC (0.4 M, each), for activation of the surface-functional groups. The surface treated nanofibers were then incubated with 3 µL of capture probe (5' CGG TTT CTC GCG CGT TTC AGC ATA TTG A 3', 1 µM, spiked-PBS aliquots) at 4 ºC for 12 hours. Afterwards, the devices were carefully rinsed in DI water, and air dried under room temperature. The non-specific binding sites were later blocked with Bovine serum albumin (BSA). For DNA-hybridization, probe modified electrodes were incubated in 3 µL of the target DNA (5' TCA ATA TGC TGA AAC GCG CGA GAA ACC G 3', spiked-PBS aliquots) for 1 hour, at 37 ºC. Post hybridization, the electrodes were washed with PBS buffer and air dried, prior to further analysis.

III. Results And Discussion

A. Characterization of PANi Nanofibers

Scanning electron microscopy (SEM) images of the the wet chemically synthesized PANi nanofibers are shown in Fig. 1(a-b). The nanofibers, synthesized by a protocol described earlier, were collected as a dark green precipitate, and were then analysed using SEM. As can be seen, the fibers appear to be tens of nanometres in diameter, and comparably much larger in length, extending up to a few microns. This length to diameter proportion is important, as this ensures the

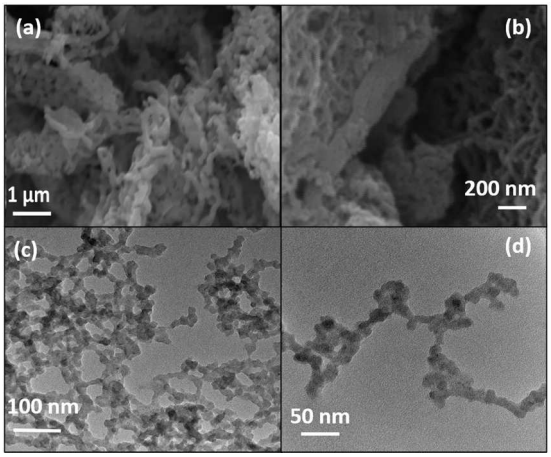

Fig. 1. SEM images (a-b) and (c-d) TEM images wet-chemically synthesized PANi nanofibers.

formation of quasi 1-D structures, creating a large surface to volume ratio. TEM images of the nanofibers are presented in Fig. 1(c-d), with different magnifications. As can be seen, the nanofiber sample has long cylindrical features, with diameter varying in the range of 10-30 nm. FTIR analysis results for bare and surface functionalized PANi nanofibers are shown in Fig. 2. Here, for the bare nanofibers, the characteristic peaks are present in the range of 500 – 1500 cm^{-1}, which can be assigned to C = C, -CN, -CH, -NH bonds. In the FTIR spectra of the surface functionalized PANi nanofibers, peaks between 1500 – 1700 cm^{-1} can be attributed to the stretching vibrations of C = O & C = C bonds, whereas the broad transmittance peak in the range of 3000 - 3500 cm^{-1} can be attributed to -OH groups.

The I~V characterization of the PANi nanofibers was performed using a Keithley 4200 SCS parametric analyser and an Agilent B1500 parametric analyser, coupled with a Cascade Summit 11K dc probe station. In this context, it is worthwhile to note, as opposed to the electrospun PANi/PEO nanofibers presented previously in [11,14], the PANi nanofibers are significantly smaller in length, and hence when dropcasted across metallic electrodes, their interconnection is relatively more complex. Under the given circumstances, to create a conductive pathway across any two adjacent metallic

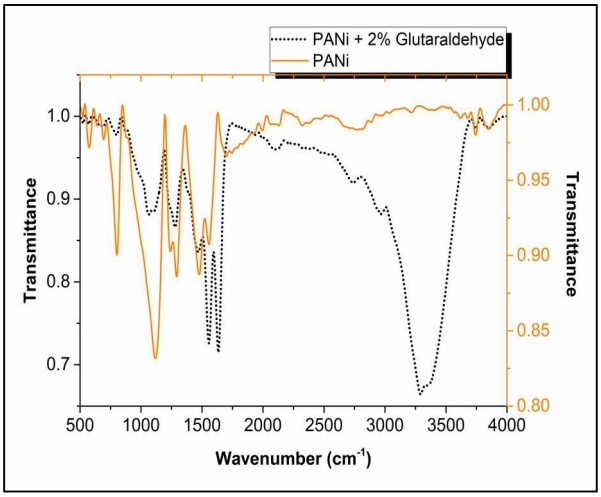

Fig. 2. FTIR analysis of wet-chemically synthesized PANi nanofibers before (bold-line) and after (dotted-line) glutaraldehyde treatment.

fingers of the used interdigitated structure, the interconnected nanofiber network must at least cover the inter-electrode gap (the shortest path). Such an elongated network of nanofibers is characterized by multiple inter-fiber crossovers and junctions. In the literature, such complexes have been attributed to several nanoscale phenomena, which influence the conductivity of the network [17-21]. It has been suggested in literature, that the electron states in PANi nanofibers are localized, and the carrier transport happens via variable range hopping [22]. In general, such localization of the electron states in the 1-D PANi nanofibers can be attributed to the interaction between the backward scattered and the forward moving electrons. Interestingly, the forward moving electrons in the individual polymer chains can hop into nearby chains, before encountering collision with the backward scattered carriers. This inter-chain coupling helps suppress the effect of 1-D localization in PANi nanofibers. Also, for a network of nanofibers, understanding the inter-fiber hopping transport is essential, for getting a comprehensive idea about the overall charge-transfer process.

In Fig. 3, the I-V characteristics of a few PANi nanofiber derived devices (D1 to D5) (nanofiber dispersion of 0.3 mg/mL), recorded in the applied bias range of -10V - +10 V, are shown. The I-V response is nearly symmetric about the vertical axis, indicating non-rectifying behaviour. The characteristics, however, is not Ohmic over the entire range of applied bias, and the near-linearity is largely confined to the lower values. The enlarged view shown in the Inset to Fig. 3, clearly reveals the crossover between the near-Ohmic and the power-law dominated regions. Keeping such behaviour in mind, in this work, for all reported sensing applications, the device resistance was calculated strictly in the linear region (i.e. -0.5 V < V_{bias} < 0.5 V) of the transfer-characteristics. Also, in doing so, we have limited the analysis only to +ve voltages, so as to avoid any inherent hysteresis and zero-crossing issues. This allows one to calculate the overall device resistance as an average quantity, using the standard Ohmic relation, without considering the region of non-linearity.

B. DNA Hybridization detection

For the envisaged DENVCP detection, device resistances were calculated (as described in the previous section) for the probe-DNA modified sensors, before and after target DNA hybridization. Subsequently, the normalized change in device resistance (ΔR/R) was estimated, where ΔR is the difference

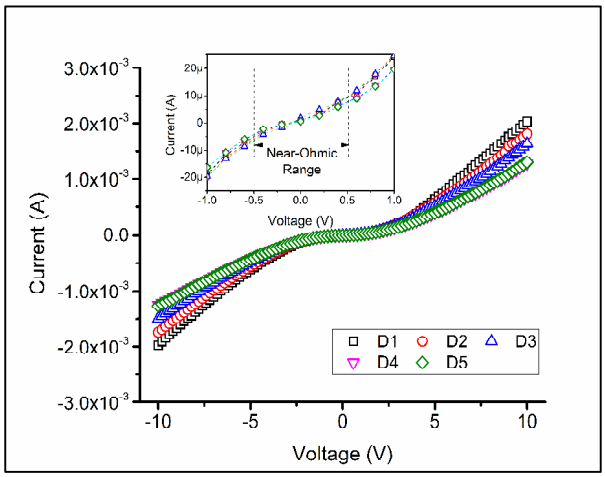

Fig. 3. I-V characteristics of PANi nanofibers. (Inset- Enlarged view.)

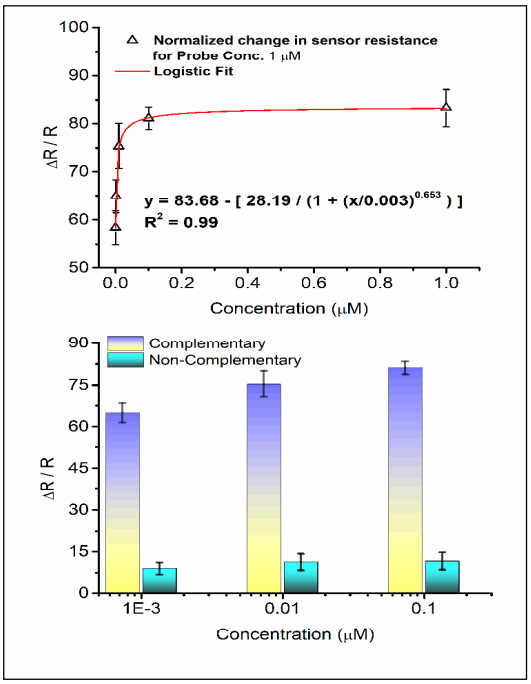

Fig. 4. Calibration curve for the DENVCP target DNA detection using the PANi nanofibers, with a four-parameter logistic curve fitting (Top). Selectivity analysis at different concentrations of complementary and non-complementary targets (Bottom).

between the device resistance with single stranded probe and the double stranded hybridized duplex, and R is the device resistance with the probe-DNA. Here, hybridization of the target DNA enhances the overall negative surface charge on the PANi nanofibers. In an analogy, this incremental negative surface charge on the conducting nanofibers can be viewed as a controlling gate potential, which in turn dictates the motion of charge carriers inside the fibers. Consequently, the overall device resistance gets modified, which can be directly correlated with the target concentration. At this point, it is worthwhile to note in the context of bioanalyte detection with chemiresistive sensors, that the overall surface charge generated in response to any analyte binding is strongly dependent on the pH. The analyte may be positively or negatively charged based on its iso-electric point and the buffer pH, and therefore, the corresponding surface charge can be either positive or negative, which in turn, may increase or decrease the device resistance proportionately.

In Fig. 4, a calibration curve for the PANi nanofiber-based devices is provided, which correlates ΔR/R to the DENVCP target DNA concentration (100 pM – 1 μM). Here, the error bars indicate standard deviation values corresponding to three identical sensing interfaces. Also, in Fig. 4, a four-parameter logistic fit is provided, with the derived calibration equation. Using the slope of the calibration graph, and the standard deviation of the blank response, the limiting detection of the sensing interface was estimated to be 6.47 pM. Furthermore, in Fig. 4, a bar diagram is provided, comparing the device's response to identical concentrations (1 nM, 10 nM and 100 nM) of complementary and non-complementary (5' TGC AGA AAA TCT TAG TGT CCC ATC TG 3') target DNAs, so as to establish the specificity of the sensing interface.

IV. Conclusion

In this paper, the fabrication of chemiresistive biosensing platforms using wet-chemically synthesized PANi nanofibers, and their application in Dengue virus specific consensus primer detection is reported. Further, current-voltage behaviour of the dropcasted nanofiber-networks were studied, and discussed in detail. When subjected to target DNA detection in the concentration range of 100 pM – 1 μM, the chemiresistors accounted for a limiting detection of 6.47 pM. The sensing results presented in this work, however, were limited only to spiked-buffer samples. Understandably, it is essential to investigate the performance of the said sensors against real-time patient samples, and the future scope of this work is aimed in that direction.

Acknowledgment

The authors would like to thank the 'Department of science and technology, Fund for improvement of S&T infrastructure' (DST-FIST), Ministry of Electronics and Information Technology (MeitY), Government of India for funding this research.

References

[1] E. M. Boon, D. M. Ceres, T. G. Drummond, M. G. Hill, and J. K. Barton, "Mutation detection by electrocatalysis at DNA-modified electrodes," Nature biotechnology, vol. 18(10), pp. 1096, 2000.

[2] N. P. Gerry, N. E. Witowski, J. Day, R. P. Hammer, G. Barany, and F. Barany, "Universal DNA microarray method for multiplex detection of low abundance point mutations," Journal of molecular biology, vol. 292(2), pp. 251-262, 1999.

[3] O. P. Kallioniemi, A. Kallioniemi, J. Piper, J. Isola, F. M. Waldman, J. W. Gray, and D. Pinkel, "Optimizing comparative genomic hybridization for analysis of DNA sequence copy number changes in solid tumors," Genes, Chromosomes and Cancer, vol. 10(4), pp. 231-243, 1994.

[4] J. C. Alwine, D. J. Kemp, and G. R. Stark, "Method for detection of specific RNAs in agarose gels by transfer to diazobenzyloxymethyl-paper and hybridization with DNA probes," Proceedings of the National Academy of Sciences, vol. 74(12), pp. 5350-5354, 1977.

[5] A. Abbaspour, F. Norouz-Sarvestani, A. Noori, and N. Soltani, "Aptamer-conjugated silver nanoparticles for electrochemical dual-aptamer-based sandwich detection of staphylococcus aureus," Biosensors and Bioelectronics,vol. 68, pp. 149-155, 2015.

[6] M. Prado, I. Ortea, S. Vial, J. Rivas, P. Calo-Mata, and J. Barros-Velázquez, "Advanced DNA-and protein-based methods for the detection and investigation of food allergens," Critical reviews in food science and nutrition, vol. 56(15), pp. 2511-2542, 2016.

[7] M. B. Gumpu, S. Sethuraman, U. M. Krishnan, and J. B. Rayappan, "A review on detection of heavy metal ions in water–an electrochemical approach," Sensors and actuators B: chemical, vol. 213, pp. 515-533, 2015.

[8] T. G. Drummond, M. G. Hill, and J. K. Barton, "Electrochemical DNA sensors," Nature biotechnology, vol. 21(10), pp. 1192-1199, 2003.

[9] J. Zhai, H. Cui, and R. Yang, " DNA based biosensors," Biotechnology advances, vol. 15(1), pp. 43-58, 1997.

[10] S. Tripathy, S. R. K. Vanjari, V. Singh, S. Swaminathan, and S. G. Singh, "Electrospun manganese (III) oxide nanofiber based electrochemical DNA-nanobiosensor for zeptomolar detection of dengue consensus primer," Biosensors and Bioelectronics, vol. 90, pp. 378-87, 2017.

[11] S. Tripathy, A. Naithani, S. R. K. Vanjari, and S. G. Singh, "Electrospun polyaniline nanofiber based chemiresistive nanobiosensor platform for DNA Hybridization detection," In IEEE SENSORS Conference, pp. 1-3, November 2017.

[12] S. Tripathy, R. Gangwar, P. Supraja, A. N. Rao, S. R. K. Vanjari, and S. G. Singh, "Graphene Doped Mn_2O_3 Nanofibers as a Facile Electroanalytical DNA Point Mutation Detection Platform for Early Diagnosis of Breast/Ovarian Cancer," Electroanalysis, vol. 30(9), pp. 2110-20, 2018.

[13] S. Tripathy, J. Joseph, S. R. K. Vanjari, A. N. Rao, and S. G. Singh, "Flexible ITO Electrode with Gold Nanostructures for Femtomolar DNA Hybridization Detection," IEEE sensors letters. Vol. 2(4), pp. 1-4, 2018.

[14] S. Tripathy, V. Bhandari, P. Sharma, S. R. K. Vanjari, and S. G. Singh, "Chemiresistive DNA hybridization sensor with electrospun nanofibers: A method to minimize inter-device variability," Biosensors and Bioelectronics, vol. 133, pp. 24-31, 2019.

[15] S. Tripathy et al., "Miniaturized electrochemical platform with integrated PDMS reservoir for label-free DNA hybridization detection using nanostructured Au electrodes," RSC Analyst. Vol. 144, pp. 6953-6961, 2019.

[16] X. Zhang, W. J. Goux, and S. K. Manohar, "Synthesis of polyaniline nanofibers by nanofiber seeding," Journal of the American Chemical Society, vol. 126(14), pp. 4502-4503, 2004.

[17] Y. Zhang, and G. C. Rutledge, "Electrical conductivity of electrospun polyaniline and polyaniline-blend fibers and mats," Macromolecules, vol. 45(10), pp. 4238-4246, 2012.

[18] S. B. Kondawar, M. D. Deshpande, and S. P. Agrawal, "Transport properties of conductive polyaniline nanocomposites based on carbon nanotubes," Int. J. Compos. Mater, vol. 2(3), pp. 32-36, 2012.

[19] C. Nath, and A. Kumar, "Fractal like charge transport in polyaniline nanostructures," Physica B: Condensed Matter, vol. 426, pp. 94-102, 2013.

[20] H. Gu et al., "Electrical transport and magnetoresistance in advanced polyaniline nanostructures and nanocomposites," Polymer, vol. 55(17), pp. 4405-4419, 2014.

[21] M. Gosh, A. Barman, A. K. Meikap, S. K. De, and S. Chatterjee, Hopping transport in HCl doped conducting polyaniline," Physics Letters A, vol. 260(1-2), pp. 138-148, 1999.

[22] J. T. Li, Y. C. Lu, S. B. Jiang, Y. L. Zhong, and J. M. Yeh, "Phase diagram of hopping conduction mechanisms in polymer nanofiber network," Journal of Applied Physics, vol. 118(21), pp. 215104, 2015.